

The Effect of an Electric Field on Optical Spectra in Electronic Structures of $\text{Si-Si}_{1-x}\text{Ge}_x$ Quantum well

Dr. Jamal S. Elfurdag
Physics Department, Faculty of Science
Zawia University

Abstract:

In this paper we apply technique to strained quantum well structures, and to show the effect of strong external electric field up to $5 \times 10^5 \text{ Vcm}^{-1}$ upon electronic structure and optical spectra of $\text{Si-Si}_{1-x}\text{Ge}_x$ quantum well structures.

This will provide us with an opportunity to present the microscopic picture of optical transition probabilities and the transmission probabilities for transport between wells. We have focused on the states derived from the lowest conduction band and on the states derived from the uppermost valence band. In the absence of an external electric field and under

influence of an external electric field. We find that results differ from the predictions based on idealized models.

Introduction:

The effect of an external electric field up on electronic states in quantum well structure has received much attention in the literature of particular interest (1,2). There have been many studies of fundamental electronic and optical properties of ordered Si-Ge heterostructures (3). The effect of an external electric field upon the optical spectra of quantum well and superlattices structures has been studied both theoretically and experimentally (4). However, theoretical modeling has usually been carried out in the framework of a "particle in a box" model. In order to model the effect of an external electric field in Si-Ge quantitatively, it is necessary to describe the electronic structure of a very large supercell which may contain thousands of atoms. At the same time one must be able to represent correctly the key features of the electronic structure near the band edges.

It is important to examine field induced changes in the optical spectra. In an isolated well, we would expect the principal transition to be red shifted since the localization of the wavefunction would not change much except in very high electric fields and the gap between the conduction and valence levels would decrease slightly. In fact the electric field was sufficiently strong and the coupling between wells was weak, then we would a blue shift rather than a red shift(5). In larger scale systems such as GaAs-AlGaAs and InAs-AlGaSb, The optical matrix elements for the strongest transitions decrease much more rapidly, usually by several orders of magnitude for electric fields of around ($5 \text{ m V}/\text{\AA}$), (6,7).

Method:

We have considered a variety of quantum well structures, with five and nine wells in each supercell. Each supercell is terminated by a thick layer of substrate material, thereby, ensuring that the interaction between them is negligibly small.

In order to create a workable computational model, we proceed, a full scale pseudopotential calculations for Si-Si_{1-x} Ge_x quantum well structures, we have described the solutions as following:-

I- In the absence of an external electric field that then used to construct the wavefunctions ψ of the stark Hamiltonian

$$\psi = \sum_{n,k} B_{n,k} \Phi_{n,k}$$

Which satisfy the Schrodinger equation

$$(H + V - E) \psi = 0$$

$$H\Phi_{n,k} = E_{n,k} \Phi_{n,k}$$

Where V represents the external electric field, in this case ($V = 0$), n, number of bands, and k, the wavevector.

II- In the presence of an external electric field, in this case ($V \neq 0$),

$$(H_0 + V - E) \psi = 0$$

as shown in figure(1).

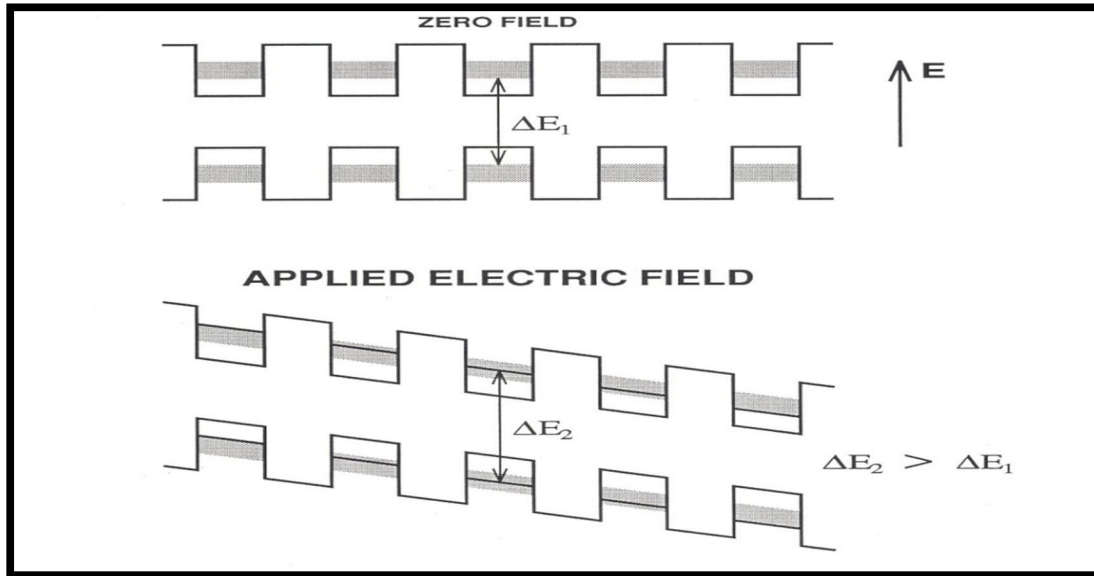


Figure (1) Shows the system with zero field ,and with applied external electric field.

Discussion and Results:

We shall look at in this paper the quantum well systems, which are all grown on a SiGe alloy substrate, this is necessary in order to avoid strain build up in large period structures. The wells and barriers are chosen to have a thickness of five monolayers, these structures have the property that the band gap is direct and has a relatively large oscillator strength. We have looked at two systems, consisting of five and nine wells.

Figure(2) Shows the unit cell for each of these structures.

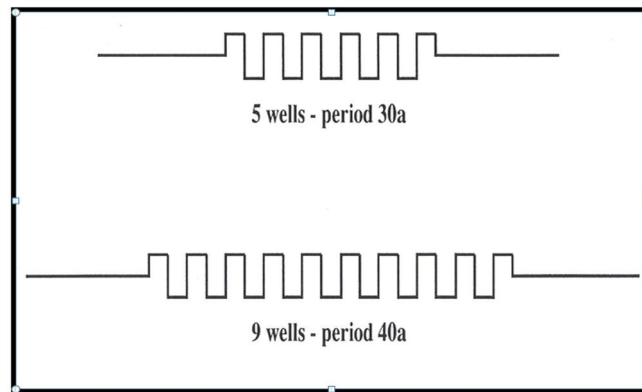


Figure (2) Shows, Unit cells for 5 and 9 wells calculations, where (a) is the bulk SiGe alloy lattice constant.

Calculations without the application of an external electric field produce the charge densities shown in figures (3,4).

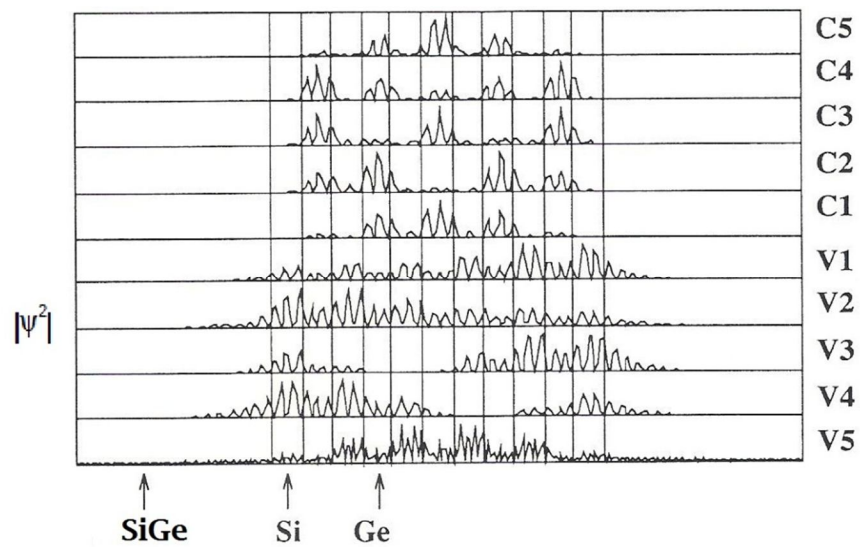


Figure (3) Shows, charge densities of lowest five conduction band states and the highest five valence band states in the absence of an external electric field for the system of five wells.

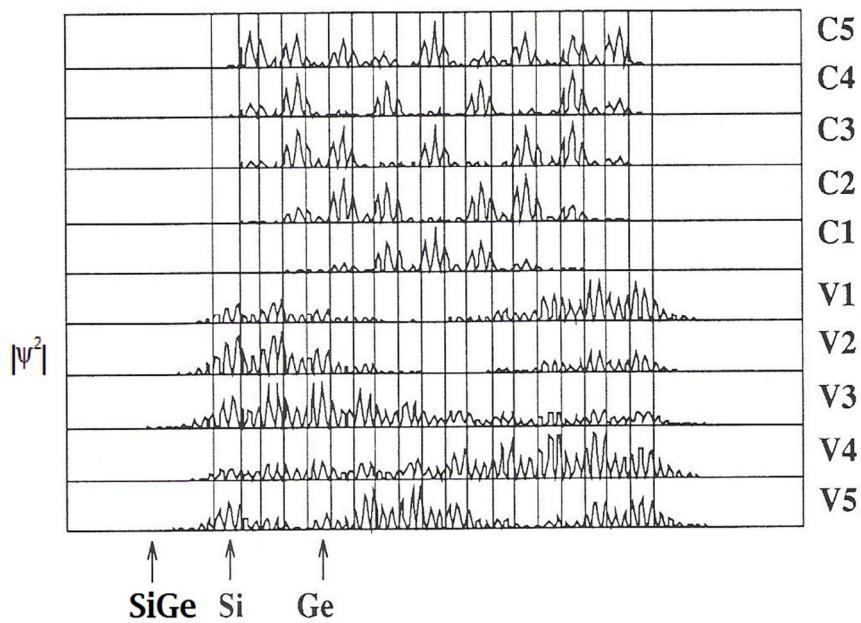


Figure (4) Shows, charge densities of lowest five conduction band states and the highest five valence band states in the absence of an external electric field for the system of nine wells.

For each system we have plotted the charge densities ($|\psi^2|$) for the top 5 valence states and lowest 5 conduction states.

We have imposed fields up to $5 \times 10^5 \text{ Vcm}^{-1}$ on a system consisting of five wells, and shows how the energy levels vary with applied external electric field. Figure (5), shows the lowest ten conduction band states and the top thirteen valence states.

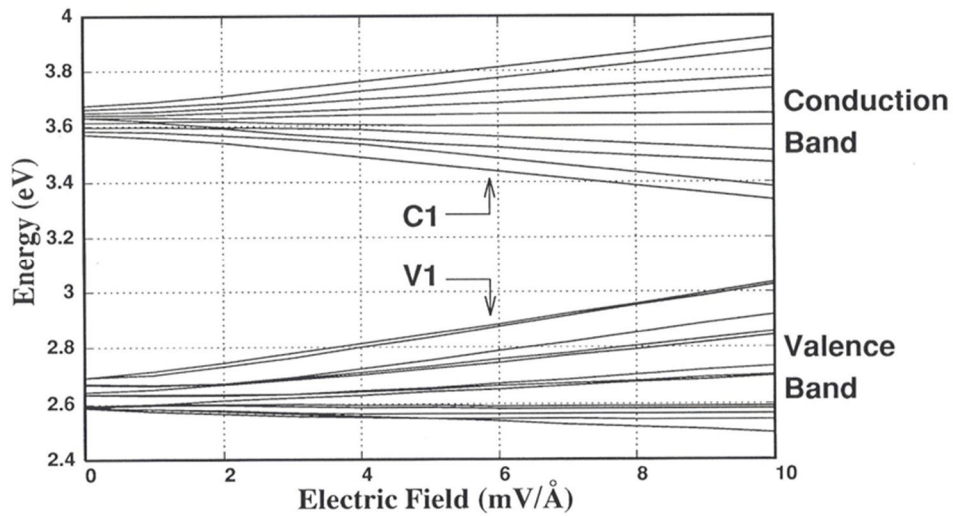


Figure (5) Shows, energy band dispersions for five well system. And the Stark ladder and the quasi double degeneracies the conduction band states .

In the conduction states, the stark ladder is clearly evident, the quasidouble degeneracy of the conduction states is shown by the fact that the energy levels fan out in pairs for higher values of the electric field. The energy level diagram shows that for the conduction band states, the linear behavior associated with wave packet localization in individual wells does not begin until the external electric field has reached approximately $4 \times 10^5 \text{ Vcm}^{-1}$. The top valence states move upwards whereas the bottom conduction states move downwards, this upward movement of the valence states is accompanied by a shift in the localization of the wavefunctions in the opposite direction to that of the conduction wavefunctions charge densities for these states in both the linear and non-linear regimes are shown in figures(6,7,8).

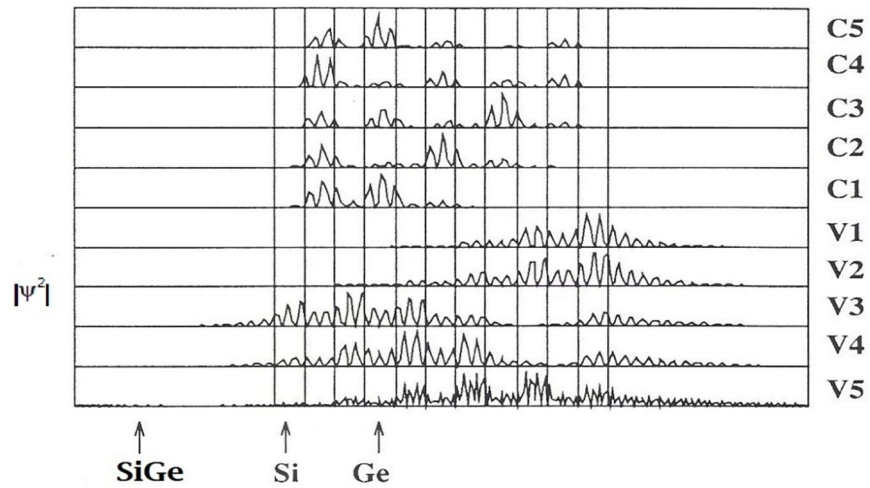


Figure (6), Shows charge densities for the states nearest the band edge in the five well system with an external electric field of $1 \times 10^5 \text{ Vcm}^{-1}$.

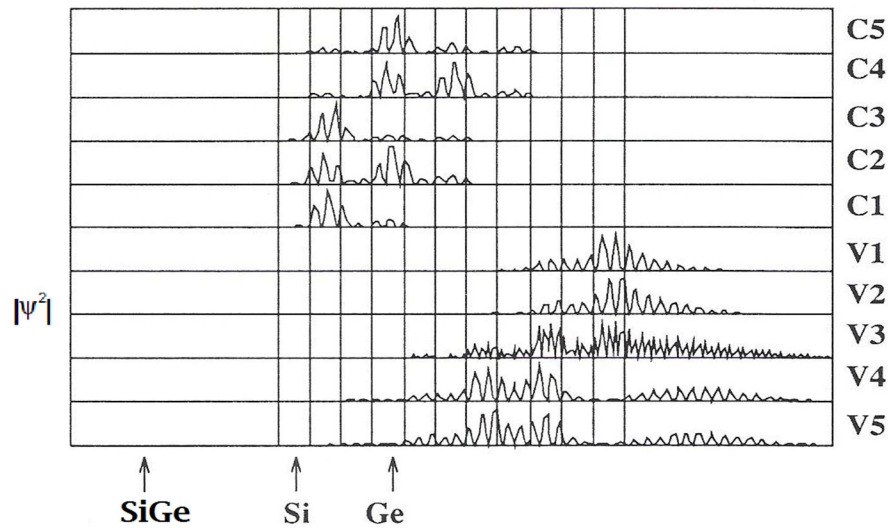


Figure (7), Shows charge densities for the states nearest the band edge in the five well system with an external electric field of $3 \times 10^5 \text{ Vcm}^{-1}$.

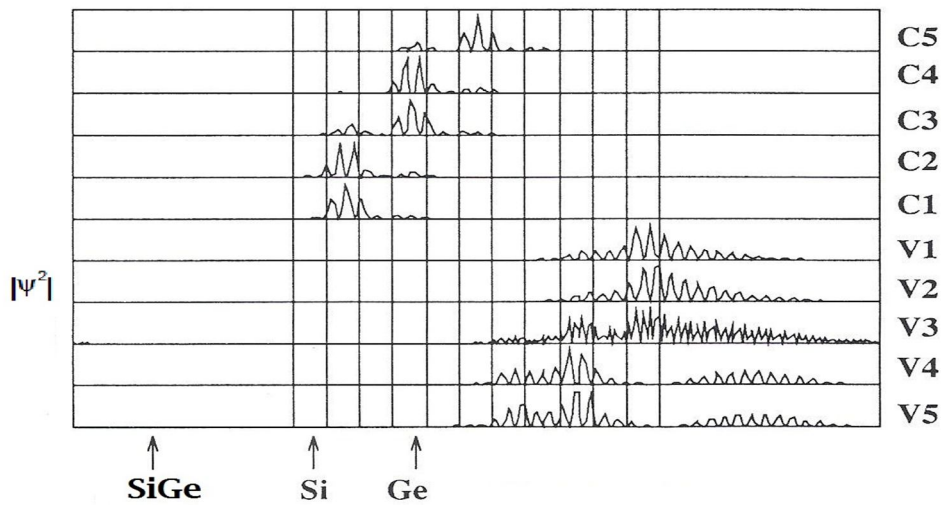


Figure (8), Shows charge densities for the states nearest the band edge in the five well system with an external electric field of $5 \times 10^5 \text{ Vcm}^{-1}$.

As we expect from the energy field relationship, the states do not become fully localized in the individual wells until the electric field is about $5 \times 10^5 \text{ Vcm}^{-1}$. Further increases in the electric field beyond this value do not alter the charge densities much. The valence states are not as well localized as the conduction states, this is due to the much smaller effective masses in the valence band for both heavy and light holes.

When we go to a system consisting of nine wells, the dimensions of the structure increase dramatically. One effect of this is that for a given electric field, the potential drop across the well is now much greater, the energy level diagram in figure (9), shows that for electric field around $8 \times 10^5 \text{ Vcm}^{-1}$, the valence and conduction bands cross, again, at high electric fields the quasidouble degeneracy of the conduction states causes the levels to fan out in pairs.

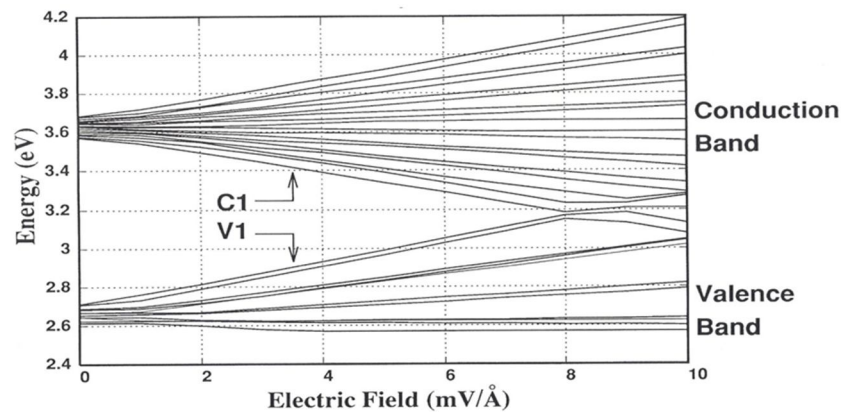


Figure (9) Shows, energy band dispersions for nine well system. And the Stark ladder and the quasi double degeneracies the conduction band states .

Since the dimensions of the structure are now much larger than in the five well case, the dispersion induced by the electric field in the valence and conduction bands is greatly increased. The charge densities in figures (10,11,12) are qualitatively similar to those we obtained in the five well case.

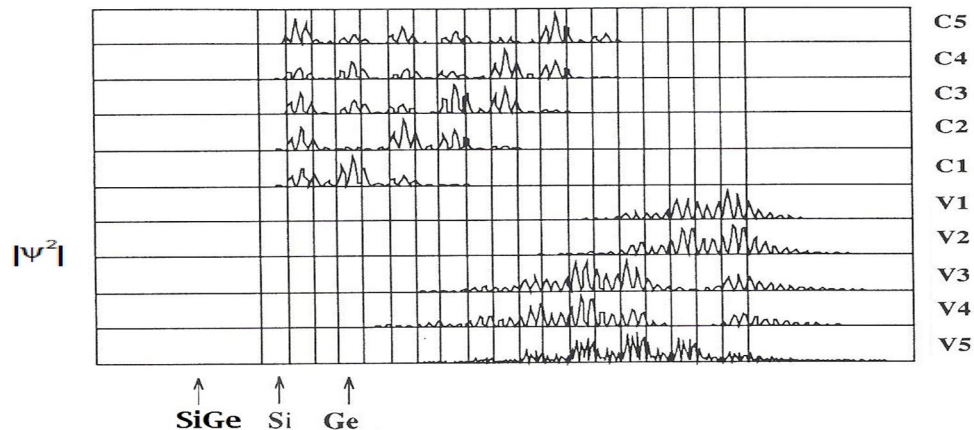


Figure (10), Shows charge densities for the states nearest the band edge in the nine well system with an external electric field of $1 \times 10^5 \text{ Vcm}^{-1}$.

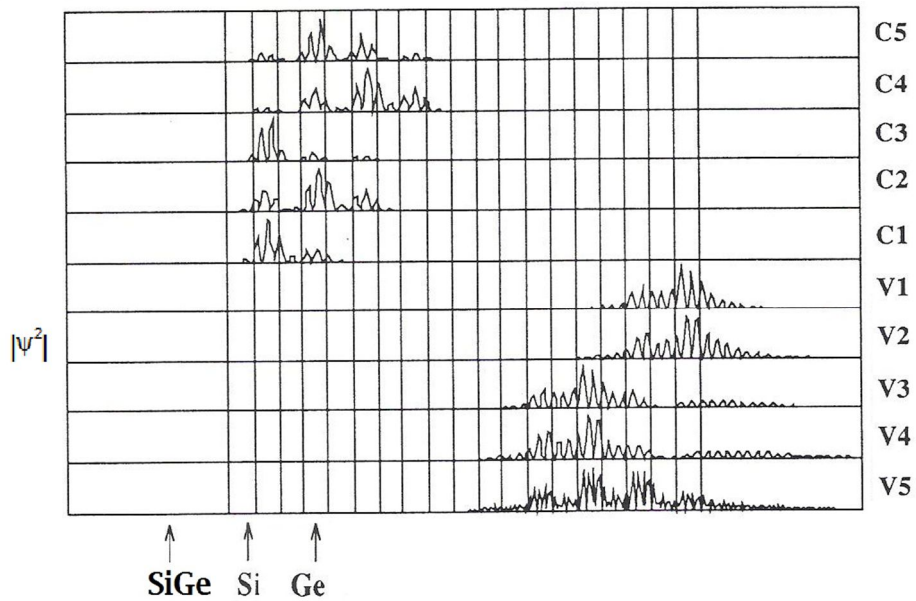


Figure (11), Shows charge densities for the states nearest the band edge in the nine well system with an external electric field of $3 \times 10^5 \text{ Vcm}^{-1}$.

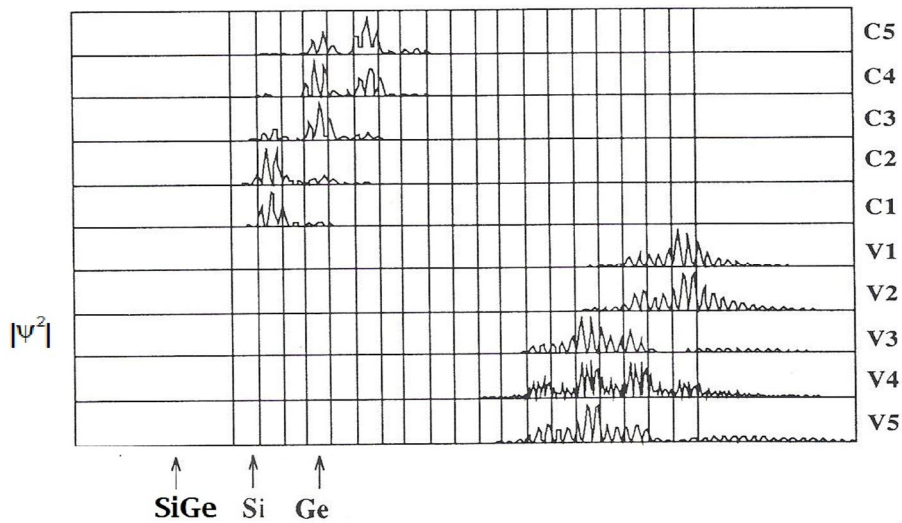


Figure (12), Shows charge densities for the states nearest the band edge in the nine well system with an external electric field of $5 \times 10^5 \text{ Vcm}^{-1}$.

The main difference is that the linear regime takes rather longer to reach. This can be seen by noting that the localization of the conduction states at a electric field strength of $5 \times 10^5 \text{ Vcm}^{-1}$ is not as great as in the five well case.

The optical matrix element for lowest energy transition across the band gap is plotted against the electric field in figure (13). It is seen that as the electric field increases, the magnitude of the optical matrix element decreases. This decrease is caused by the decreasing spatial overlap between the lowest conduction states and the highest valence state. In fact the principal across the gap transition in our system is rather stronger at zero electric field, this is due to the double degeneracy of the heavy hole state at the top of the valence band which effectively doubles the transition strength. This is true in two systems we are considering since they all exhibit a double degeneracy at the top of the valence band. Since the coupling between wells is still relatively strong, the size of the optical element is not reduced sufficiently to make the transition forbidden, hence we predict a red shift, at least for small electric fields.

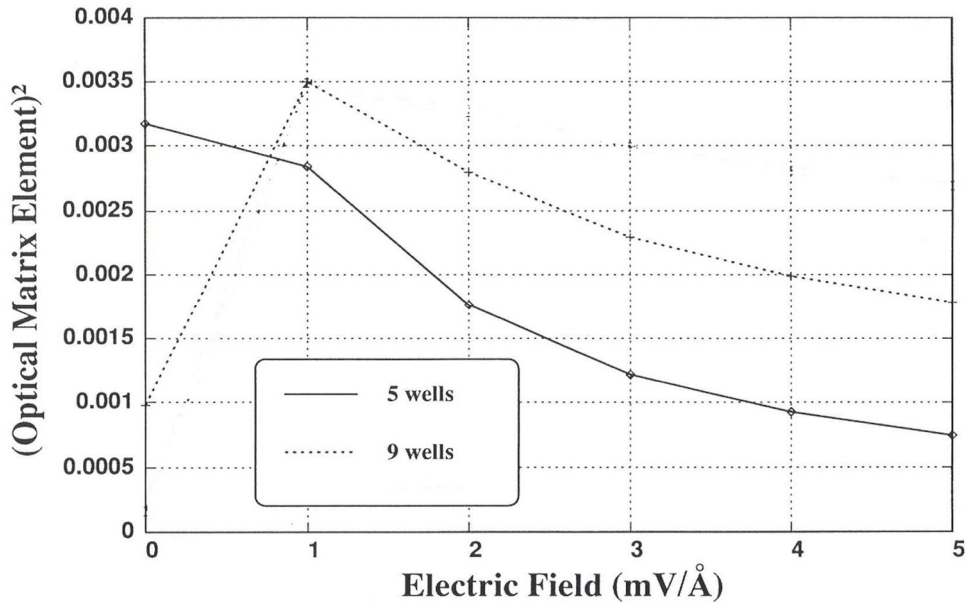


Figure (13), Shows the variation of the lowest energy transition across the gap as a function of applied field for the five well and nine well systems. (square of the optical matrix element for $V1 \rightarrow C1$ transition)

In the case of nine wells, this transition is actually enhanced by the application of a small electric field, this enhancement is a consequence of the fact that initially, there is little overlap between the top valence states and the lowest conduction states at zero electric field, as can be seen from the charge densities in figure(3). Increasing the electric field beyond about $1 \times 10^5 \text{ Vcm}^{-1}$ however, starts to reduce the strength of the transition, at zero field the transition is much lower than was the case for five wells. In fact, the rate of decrease in transition strength is slightly lower than was the case for five wells.

Conclusions:

We have employed relativistic pseudopotentials to model the effect of an external electric field of up to $5 \times 10^5 \text{ Vcm}^{-1}$ on the electronic

structure and optical spectra of Si-Si_{1-x} Ge_x quantum well structures. Calculations of energies, wavefunctions and optical matrix elements was carryout for states near the band edges in two related SiGe quantum well structures, we find that our results differ significantly from the predictions based on idealized models. This is because in a strained layer structure characterized by a set of closely spaced levels near the band edges originating from different bulk bands, the field induced momentum mixing sets in at relatively low electric fields and its effect upon near-forbidden transitions is strong. This affects the form of Stark shifts, the mixing of waves of different bulk momenta which breaks selection rules, and the transmission coefficients. Our results indicate that an applied external electric field should produce a red shift in the observed band gap.

References:

- 1- Dignam M. M. and Sipe J. E. (1991), *Phys. Rev. B* **43** 4097.
- 2- Grimmeiss H. G. ,Nagesh V. , Presting H. ,Kibbel K. and Kasper E. (1992), *Phys. Rev. B* **45** 1236.
- 3- Jaros M. , *Semiconductors and Semimetals*, (1990), **32**, 175.
- 4- Hagon J. P. and Jaros M. , (1990), *Phys. Rev. ,B*, **41**,2900.
- 5- Jaros M. ,Beavis A. W. , Hagon J. P. , Turton R. J. , Miloszewski A. and Wong K. B. , (1992), *Thin Solid Films*, **222**,205.
- 6- Elfardagh J.,(2004),*University Bulletin, Al-zawia University*, **6**,45
- 7- Corbin E. ,Wong K. B. and Jaros M. ,(1994), *Phys. Rev. B* **50**,2339.
- 8- Elfardagh J. ,(2002),*University Bulletin, Al-zawia University*, **4**,21.
- 9- Rieger M. M. and Vogl P. ,(1993), *Phys. Rev. B* **48**, 14276.